

Numerical Experiments with Multi-Models for Paleo-Environmental Problems

Project Representative

Ayako Abe-Ouchi Atmosphere and Ocean Research Institute, The University of Tokyo

Authors

Ayako Abe-Ouchi^{*1}, Masakazu Yoshimori^{*1}, Wing-Le Chan^{*1}, Akitomo Yamamoto^{*1},
Kazumi Ozaki^{*1}, Ryouta O'ishi^{*2}, Mika Ichino^{*2}, Yusuke Ozawa^{*1}, Takashi Obase^{*1},
Sam Sherriff Tadano^{*1}, Nitta Tomoko^{*1} and Alexandre Laine^{*2}

*1 Atmosphere and Ocean Research Institute, The University of Tokyo

*2 National Institute of Polar Research, Research Organization of Information and Systems

The MIROC4m AOGCM was used for several paleoclimate simulations of the mid-Pliocene Warm Period (mPWP, 3.3-3.0 million years ago), stadial states (millennial-scale cold period during the last glacial cycle), and the last millennium (850-2000 C.E.). MIROC4m mPWP simulations show that greenhouse gas emissivity dominates the tropical warming in all models, whereas clear-sky albedo is important in the high latitudes.

A higher resolution AGCM is used to simulate freshwater hosing to investigate stadial climate states and vegetation distribution. Initial analysis suggests that summer monsoonal changes indicated by proxy data are well-represented. Vegetation distribution shows a global pattern of decrease of forest which is similar to that of a reconstructed one. However, the intensity of decrease is underestimated.

In order to evaluate the impact of collapse of methane hydrate upon the climate, preliminary estimation has been done using MIROC3.2 quadrupled atmospheric CO₂ experiment. The result indicates that a huge amount of methane hydrate is decomposed throughout a timescale of several thousand years.

Several sensitivity experiments are conducted under time-varying forcing of the last millennium. The response pattern of the climate to extraordinarily large volcanic events suggests that the phase of the Pacific Decadal Oscillation appears to be locked to the event. This characteristic is commonly seen in different ensemble members whose integration started from different initial conditions.

Keywords: atmosphere-ocean GCM MIROC, paleoclimate modeling, mid-Pliocene, last millennium

1. Introduction

The mid-Pliocene warm period (mPWP), defined as the interval between 3.3-3.0 million years ago, was the most recent period with sustained warmth during the earth's history. Global mean temperatures were comparable to those predicted for the latter half of the 21st century, leading to the mPWP as being thought of as an analogue for future climate conditions. This particular interval was chosen for paleoclimate reconstruction for a variety of reasons, not least because there are multiple temperature proxies from extant fauna and flora and continental distribution was not unlike that of present day. The mPWP has thus become a period of particular interest within the paleoclimate community and includes potential targets, such as climate sensitivity and vegetation, for reducing uncertainties in future projections.

The Late Pleistocene age was characterized by abrupt climate change of millennial timescales, the Dansgaard-Oeschger Cycle. Within this age, MIS3 (60,000-30,000 years ago) was

an important time for the dispersal of Modern Humans. To investigate the reason for the replacement of Neanderthals by Modern Humans, the reconstruction of environmental factors, especially climate and vegetation distribution, is important. In the current study we report on the progress of the reconstruction of climate and vegetation in the Late Pleistocene using GCMs.

Global warming could decompose methane hydrate and cause methane release into the ocean. This methane release is thought to affect climate and ocean biogeochemical cycle in future and past global warming, such as the Paleocene-Eocene Thermal Maximum (PETM) (about 56 million years ago) and Ocean Anoxic Events (OAEs) in the Mesozoic (252-66 million years ago). We estimated the methane hydrate inventory loss in response to global warming and discuss its potential impact on ocean oxygen depletion. Our study is a highly suggestive estimation for both future and past climate change.

The last millennium (LM) simulation (850 – 2000 A.D.), designed under the Paleoclimate Modelling Intercomparison

Project phase 3 and included in a suite of tier 2 experiments in the Coupled Model Intercomparison Project phase 5, is now being carried out by multiple climate modeling centers across the world and archived. In the current study, we focus on the response of the Pacific Decadal Oscillation upon volcanic forcing.

2. Mid-Pliocene Warm Period: model-model and model-data comparisons

The Pliocene Model Intercomparison Project (PlioMIP) was set up in 2010 to stimulate interest in the mid-Pliocene warm period by bringing international climate modeling groups together and assessing climate simulations of that period by both model-model and model-data comparisons [1,2]. The first phase recently produced many interesting results just as a possible time slice is being identified for the upcoming next phase [3]. The MIROC4m atmosphere-ocean model had previously been used to run simulations adhering to PlioMIP guidelines [4] and recent results focus on the various aspects of model inter-comparisons and data-model discrepancies.

The MIROC4m results, as with those from other individual models, show mostly warming in the mid-Pliocene sea surface temperatures (SST). There are only two locations where the mid-Pliocene multi-model-mean value is more than 3°C higher than the present day value [5]. Most models show slight warming in the tropical regions, in contrast to many of the PRISM3 proxy data there. On the other hand, the models do not show warming in the high latitudes of the Atlantic Ocean to be as high as that suggested by proxy data. Thus, although there is a polar amplification of SSTs in model data, it appears weaker than PRISM3 data set. It is difficult to explain this by changes in ocean heat transport since models show only small changes and no consistent increase in the strength of the Atlantic meridional overturning circulation (AMOC) [6]. Energy balance calculations show that greenhouse gas emissivity dominates the tropical warming in all models, whereas clear-sky albedo is important in the high latitudes [7]. Even though greenhouse gas warming is fairly consistent at all latitudes, it is partially offset at high latitudes by the cloudy sky impact on the planetary albedo. Comparisons with confidence-assessed temperature proxy data and biome reconstructions reveal a substantial cold bias in the model surface air temperatures of the northern hemisphere, especially Siberia [8]. A more robust evaluation of the capabilities of models to simulate mid-Pliocene warming may be achieved by removing the temporal constraints on the current PlioMIP proxy records.

3. Modeling climates of the Late Pleistocene with MIROC4m AOGCM and AGCM

The Late Pleistocene lasted from the end of the previous interglacial period to the start of the warm Holocene and was characterized mostly by widespread glacial ice. It is thought

that melting sea ice or icebergs from the Laurentide ice sheet led to a large discharge of freshwater into the North Atlantic Ocean during Heinrich events and a weakening of the Atlantic meridional overturning circulation, coinciding with large fluctuations in temperature, as suggested by geochemical records of ice cores. This period also saw modern humans spread throughout the world and other remaining species of the same genus, such as the Neanderthals, become extinct. One hypothesis proposed to explain the extinction of the Neanderthals points to their inability to adapt to climate and environmental changes during oxygen isotope stage 3 (OIS-3), 58.9-27.6ka BP [9]. In order to better understand the role of climate and vegetation changes on the migration patterns of early modern humans and Neanderthals, climate models can be used to reconstruct past climates and, in particular, those of the cool stadials and warm interstadials. We analyzed the simulated climates for several versions of the MIROC model (and AOGCM, mid-resolution T42 AGCM and a high-resolution T106 AGCM) and also compared them with some proxy data.

Previous studies have shown that release of freshwater into the northern North Atlantic Ocean, akin to Heinrich events, can weaken the AMOC, affecting climate throughout Europe and beyond. To mimic this release, AOGCM simulations include ‘freshwater hosing’ whereby a freshwater flux had been applied over the northern North Atlantic [10,11]. In a mid-glacial experiment (Hosing), freshwater was released at a rate of 0.1Sv ($10^6\text{m}^3/\text{s}$) for 500 years in MIROC. In a second experiment (Non-hosing), this hosing was then switched off, resulting in a recovery in the AMOC. Sea surface temperatures and sea ice from these two experiments were applied to the mid- and high-resolution AGCM to simulate climates depicting the cool stadials and warm interstadials. This is slightly different to previous analyzes where the stage before freshwater hosing is applied was taken to represent the interstadial case.

Figures 1 and 2 show the temperature and precipitation response to freshwater hosing and a weakening of the AMOC. SST biases inherent in the AOGCM are adjusted for the AGCM experiments, and cooling and warming is seen over the North and South Atlantic Oceans, respectively, although warming occurs over Siberia due to differences in the AGCM sea ice treatment. Drier conditions during the summer as inferred from proxy data (red circles in Fig. 2) are simulated better in the AGCM, for example, near the Philippines. In all experiments, there is a weakening of the South Asian summer monsoon, as seen in the weakening of the southwesterlies and the drier conditions over the northern Arabian Sea. Adjustments made to the sea ice, such as the inclusion of interannual variability, removes the warming over Siberia; the drier conditions over the western Pacific Ocean also extend inland into East Asia (Figs. 1d and 2d). Results from these climate simulations were applied to a global dynamical vegetation model to examine changes in the natural environment.

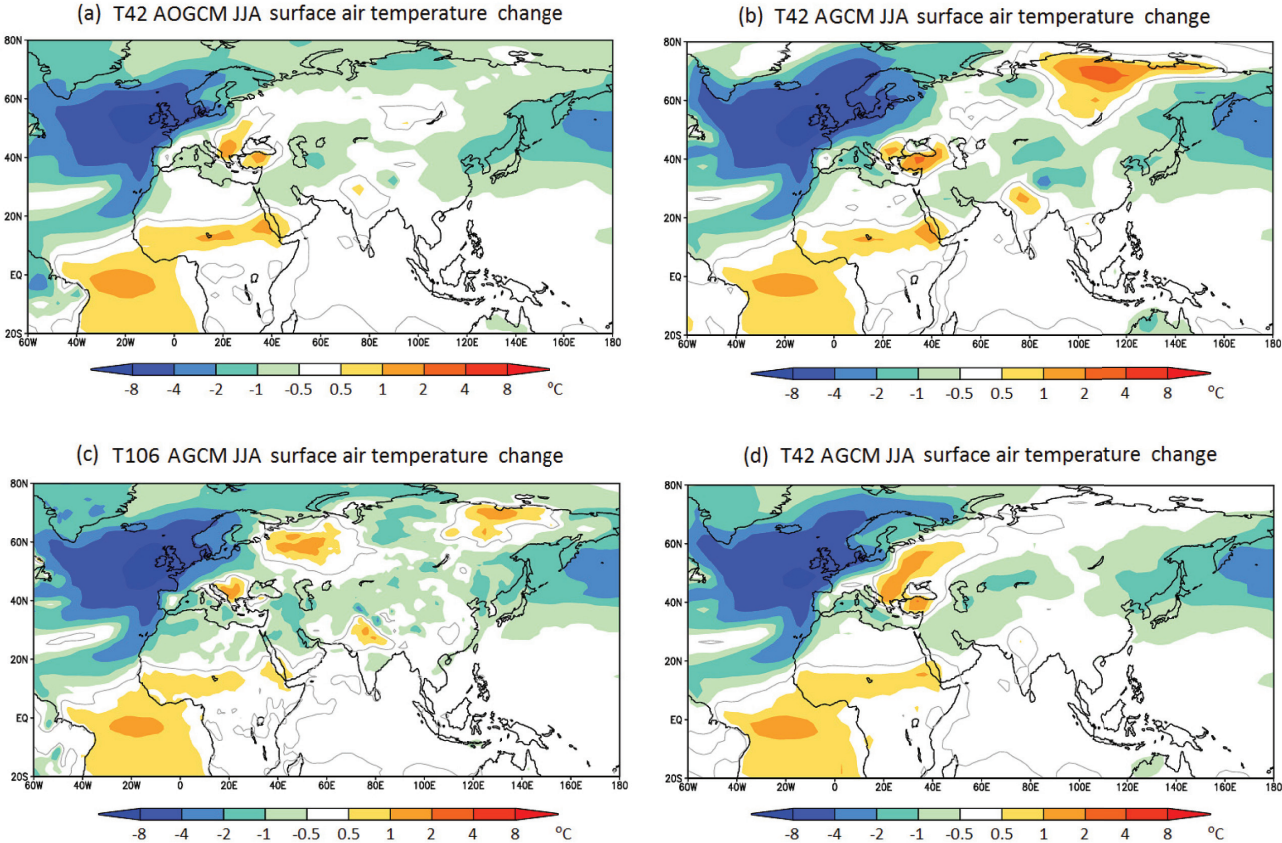


Fig. 1 Change in surface air temperature (Hosing - Non-hosing) during June-August for (a) T42 AOGCM, (b) T42 AGCM, (c) T106 AGCM and (d) T42 AGCM with adjustments made to the sea ice.

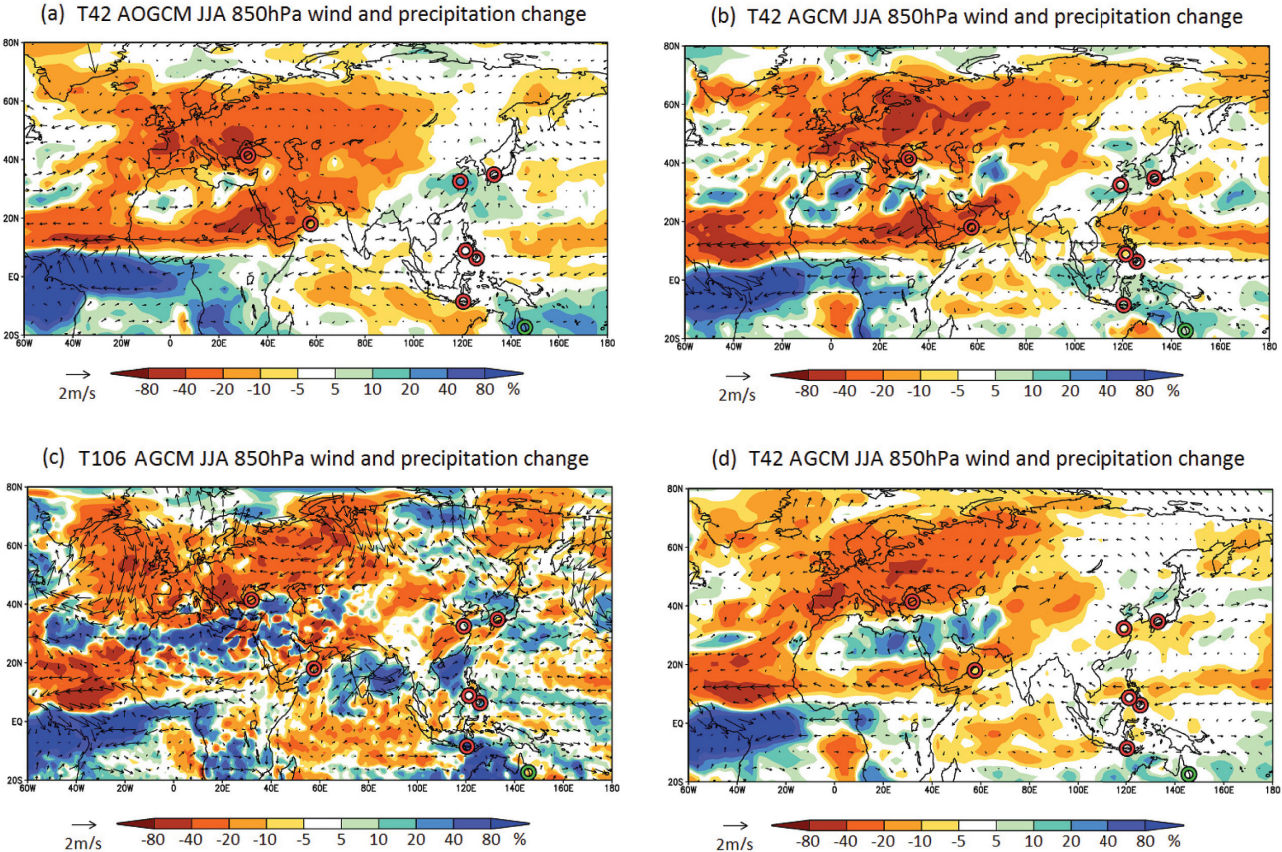


Fig. 2 Change in precipitation (Hosing/Non-hosing) and 850hPa wind (Hosing - Non-hosing) during June-August for the models as in Fig. 1. Orange and brown areas indicate drier conditions associated with freshwater hosing.

Changes in vegetation were investigated with a dynamic global vegetation model (DGVM), the Lund-Potsdam-Jena DGVM [12]. Surface air temperature and precipitation from the AOGCM were fed into the DGVM which simulates changes in plant functional types (PFT) - 8 woody/forest types and 2 herbaceous/grass types. Changes in these two are shown in Fig. 3 with bare ground as the residual. Freshwater hosing conditions tend to reduce forests throughout continental Europe, replacing them mainly with grassland. The reduction in temperature is the more dominant factor, with boreal PFTs generally surviving better in cooler conditions, but overcompensated by the decrease in temperate PFTs. There is loss of both forest and grassland over parts of Spain and northwest Africa where precipitation is greatly reduced. On the other hand, there is forest growth in the coastal regions of eastern Spain and western Italy, and across the islands in between, mainly in the form of temperate needle-leaved evergreen at the expense of grassland. This tendency of vegetation change is similar to the reconstructed vegetation change from proxies [13]. Moreover, the predicted intensity of vegetation change is the largest in Europe and less vegetation change is seen in East Asia, North America and Australia, as shown in the reconstruction. Hence, the global pattern of vegetation change is well predicted compared to the proxies. However, proxies show vegetation changes which are

more significant than those of model results. This modelling framework still underestimates vegetation change.

4. Estimations of methane hydrate inventory loss and its potential impact on ocean oxygen depletion

Increases in bottom seawater temperature due to global warming could destabilize submarine methane hydrate and cause a release of methane into the water column. The release of several thousand GtC of methane from methane hydrate decomposition may have contributed to the past global warming (e.g. PETM [14]). The methane released from the seafloor consumes dissolved oxygen via methane oxidation in seawater. Thus, massive methane release is considered as a plausible cause for OAEs in the Mesozoic, which is warmer than present climate [15]. We projected the methane hydrate inventory loss in response to global warming and discuss its potential impact on global oxygen reduction for timescales of 10kyr.

A quasi-equilibrium experiment, in which 1% annual increase in the CO₂ concentration from preindustrial values was applied until stabilization at 4 × CO₂ level after 140 years, was conducted for 3650 years with MIROC3.2 [16]. The mean bottom seawater warming with respect to preindustrial conditions was 4.5°C, and the temperature reached a quasi-

Change in vegetation fraction (Hose - Rec)

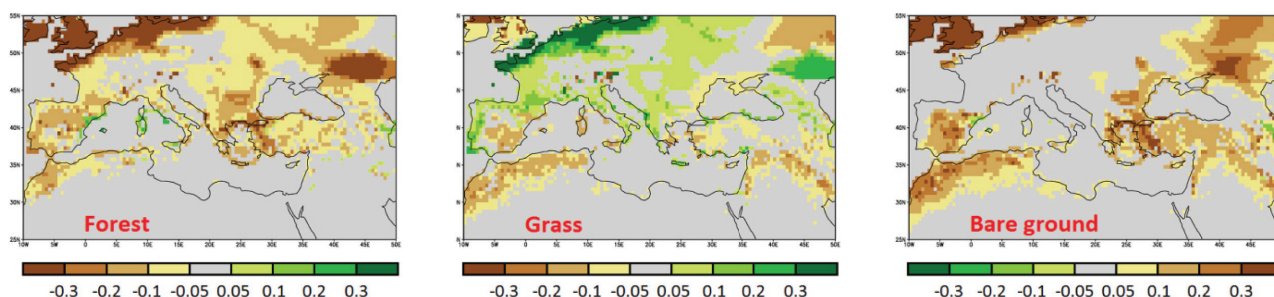


Fig. 3 The difference in vegetation fraction in LPJ dynamic global vegetation model experiments using surface air temperature and precipitation obtained from freshwater hosing and non-hosing AOGCM experiments.

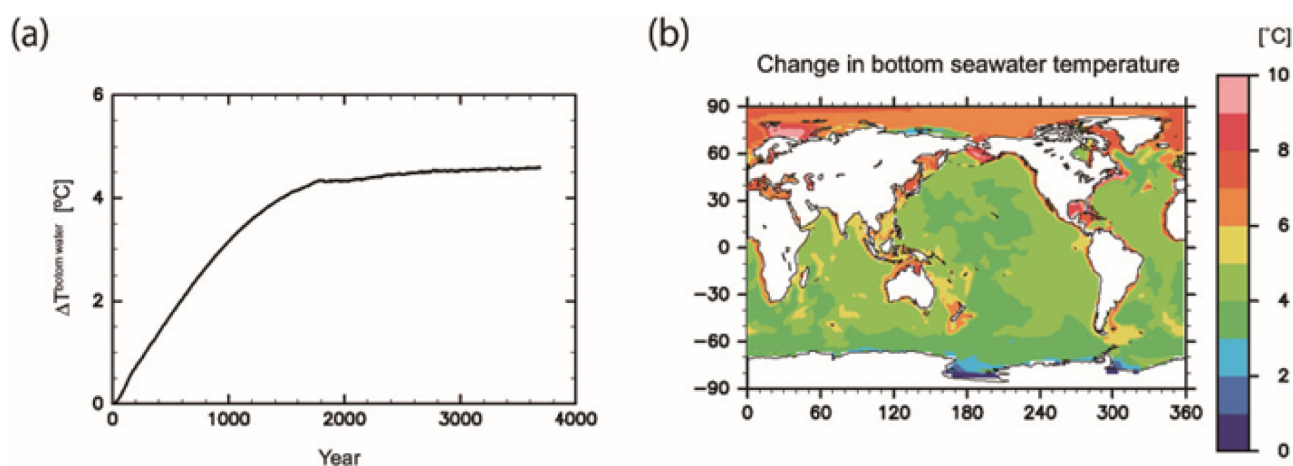


Fig. 4 (a) Temporal evolution of mean temperature changes in bottom seawater, relative to the preindustrial climate. (b) Distribution of change in the bottom seawater temperature at steady state for 4 × CO₂ experiment.

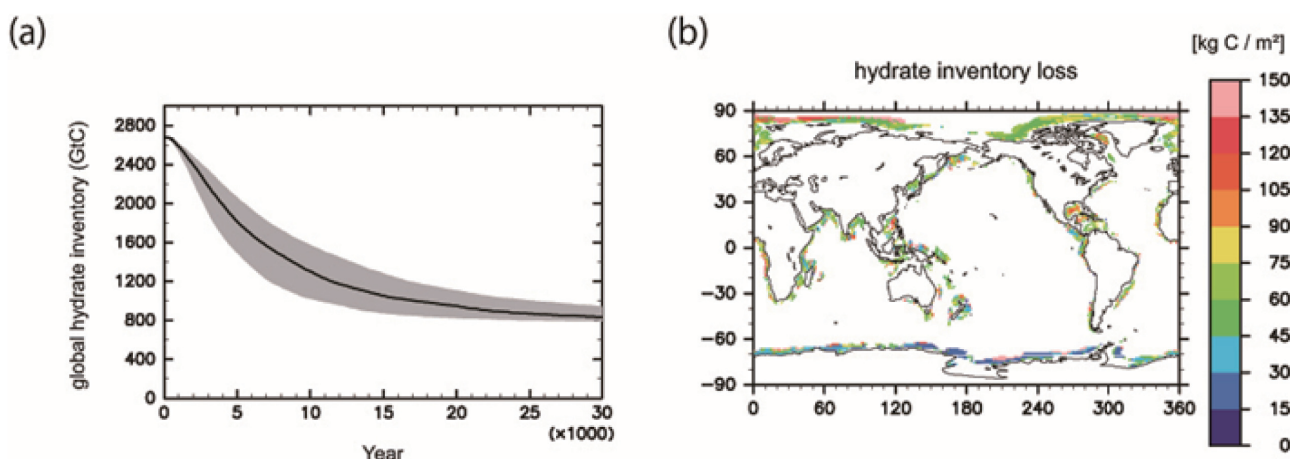


Fig. 5 (a) Temporal evolution of the global inventory of hydrates. The solid line represents the $4 \times \text{CO}_2$ experiment for hydrate evolution with thermal diffusivity of sediment of $3.0 \times 10^{-7} \text{ m}^2 \text{ s}^{-1}$. The evolution with thermal diffusivities of $1.86\text{--}4.2 \times 10^{-7} \text{ m}^2 \text{ s}^{-1}$ is indicated by the gray shading. (b) Distribution of the column-integrated inventory loss of methane hydrates at the steady state of the $4 \times \text{CO}_2$ experiment.

steady state in around 2000 model years (Fig. 4a). The bottom seawater warming in the Arctic Ocean is 2–3°C higher than that in other oceans because of polar amplifications (Fig. 4b).

We calculated the sediment warming and reduction in the global inventory of methane hydrate using calculated bottom seawater temperature, a one-dimensional thermal diffusion model and a transfer function [17]. The decomposition of methane hydrate begins to occur in the Arctic Ocean with 150 model years, and the majority of the adjustment of the hydrate inventory to the increased sediment temperatures occurs within the first 15kyr (Fig. 5a). This long timescale is primarily determined by thermal diffusion in the sediment. The global inventory of methane hydrates ultimately decreases by 1890 GtC. The hydrate inventory loss primarily occurs in the Pacific Ocean, where the hydrate inventory was found to be the greatest. A remarkable inventory loss occurs in the Arctic Ocean because the largest bottom seawater warming occurs here (Fig. 5b).

The oxidation of approximately 1200 GtC in the form of methane could potentially consume the entire oxygen content of present-day oceans. However, more than 8000 years are required to achieve a global inventory loss of 1200 GtC. Thus, because this timescale induced by slow thermal diffusion in the sediment is sufficiently longer than the timescale required for ocean ventilation (timescale of about a thousand years), the supply of oxygen from the atmosphere would be expected to prevent global ocean anoxia. The methane release in the Pacific Ocean, where present-day seawater has low oxygen concentration, would cause expansion of suboxic and hypoxic waters, having an adverse impact on marine organisms and ocean biogeochemical cycles.

5. Modeling the climate of the last millennium

Since the beginning of this project, a series of LM experiments have been carried out with the Model for Interdisciplinary Research on Climate, medium resolution

version, MIROC3.2 and MIROC4m. The result of the MIROC3.2 last millennial simulation was published by Yiou et al. (2012) [19]. MIROC4m is essentially same as MIROC3.2[16], but is renamed after a minor bug-fix on surface flux treatment over ice sheets. This fiscal year, we added two LM experiments (named R11 and R12, 13 experiments in total) of only volcanic forcing with large amplitude [18]. The two experiments differ only in the initial conditions. We focus here on the Pacific Decadal Oscillation (PDO), the leading mode of climate variability on a decadal time scale in the North Pacific. It is timely to search for the model response of PDO to external forcing as proxy records for sea surface temperature near Japan apparently sensitive to PDO are becoming available.

Figure 6 shows that MIROC4m control simulation captures the basic feature of the PDO pattern. Figure 1a corresponds to the positive phase of the PDO characterized by a cold sea surface temperature (SST) anomaly located east of Japan and by a stronger Aleutian low pressure.

We investigated the relation between volcanic forcing and PDO by the following procedures: (1) subtract SST of the perpetual 850 C.E. climatology from the simulated LM SST at each grid; and (2) subtract concurrent SST of the North Pacific (20°N–60°N, 120°E–120°W) average from the SST anomaly (obtained after the first procedure) at each grid. The first procedure is aimed at removing the effect of geographical dependence of SST spatial pattern in the unforced simulation (e.g., colder at higher latitudes), and the second procedure is aimed at removing the effect of global-scale cooling in response to volcanic forcing. Without (2), the pattern may simply exhibit domain-wide cooling, and thus it is not easy to extract the spatial SST response pattern such as PDO. Figure 7 shows the SST response pattern after the largest volcanic eruption (1258C.E.). The patterns are similar in the two experiments with different initial conditions (R11 and R12, only R11 is shown). The same analysis for the large volcanic eruption (1762C.E.) also exhibits a similar response in the two runs.

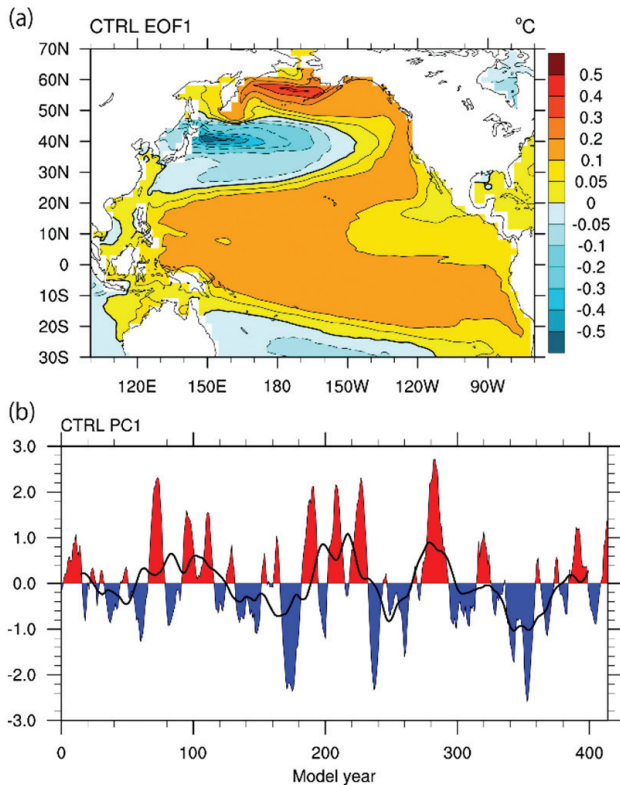


Fig. 6 The leading mode of North Pacific (20°N-60°N) sea surface temperature decadal variability in the control simulation: (a) spatial pattern; and (b) time series. Empirical orthogonal function analysis is applied after an 8-year running mean filter is imposed.

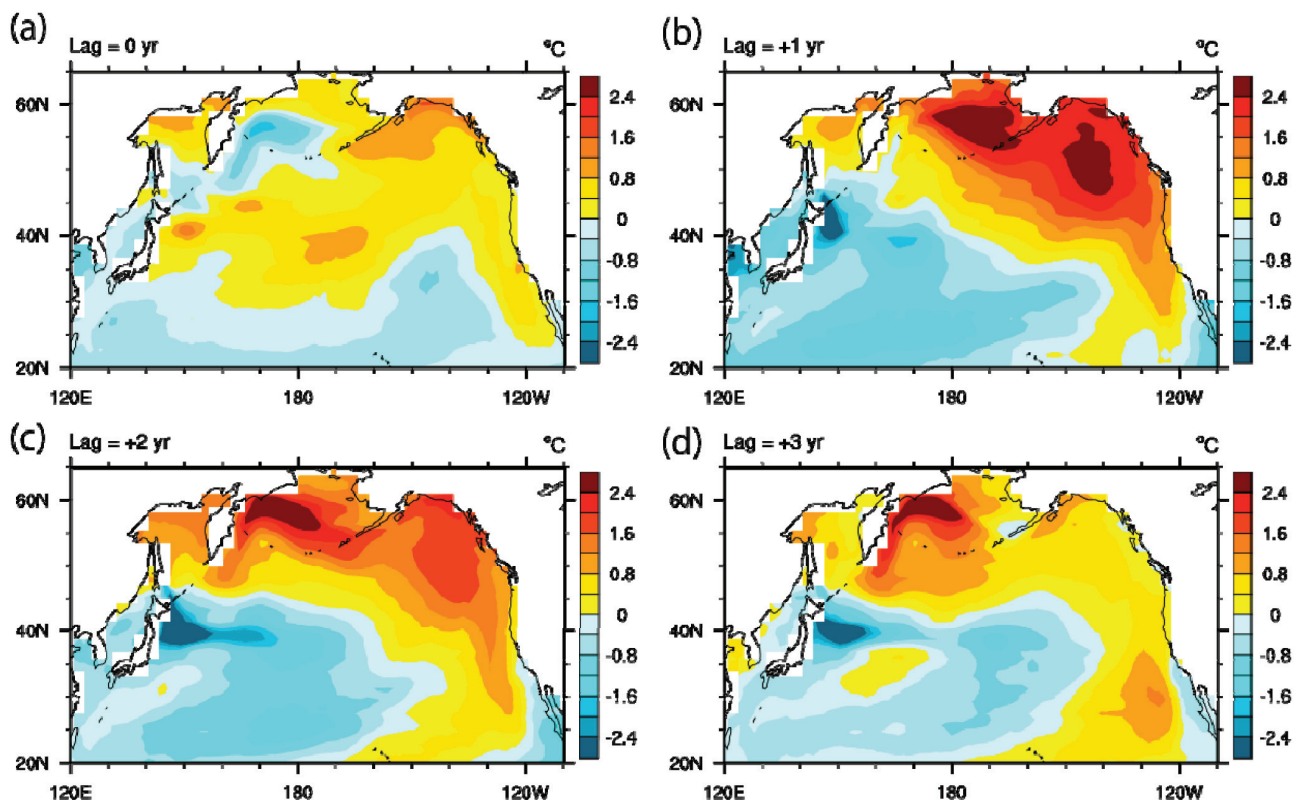


Fig. 7 Annual mean SST anomaly response pattern (R11 experiment) after the largest volcanic event (1258C.E.): (a) the year 1258; (b) 1 year later; (c) 2 years later; and (d) 3 years later. See text for the data process.

References

- [1] A. M. Haywood, H. J. Dowsett, B. Otto-Bliesner, M.A. Chandler, A. M. Dolan, D. J. Hill, D. J. Lunt, M. M. Robinson, N. A. Rosenbloom, U. Salzmann, and L. E. Sohl, Pliocene Model Intercomparison Project (PlioMIP): experimental design and boundary conditions (Experiment1), *Geosci. Model Dev.*, vol. 3, pp. 227-242, 2010; doi:10.5194/gmd-3-227-2010.
- [2] A. M. Haywood, H. J. Dowsett, M. M. Robinson, D. K. Stoll, A. M. Dolan, D. J. Lunt, B. Otto-Bliesner, and M.A. Chandler, Pliocene Model Intercomparison Project (PlioMIP): experimental design and boundary conditions (Experiment 2), *Geosci. Model Dev.*, vol. 4, pp. 571-577, 2011; doi:10.5194/gmd-4-571-2011.
- [3] A. M. Haywood, A. M. Dolan, S. J. Pickering, H. J. Dowsett, E. L. McClymont, C. L. Prescott, U. Salzmann, D. J. Hill, S. J. Hunter, D. J. Lunt, J. O. Pope, and P. J. Valdes, On the identification of a Pliocene time slice for data-model comparison, *Phil. Trans. R. Soc. A*, vol. 371: 20120515, 2013; doi:10.1098/rsta.2012.0515.
- [4] W.-L. Chan, A. Abe-Ouchi, and R. Ohgaito, Simulating the mid-Pliocene climate with the MIROC general circulation model: experimental design and initial results, *Geosci. Model Dev.*, vol. 4, pp. 1035-1049, 2011; doi:10.5194/gmd-4-1035-2011.

- [5] H. J. Dowsett, K. M. Foley, D. K. Stoll, M. A. Chandler, L. E. Sohl, M. Bentsen, B. L. Otto-Bliesner, F. J. Bragg, W. L. Chan, C. Contoux, A. M. Dolan, A. M. Haywood, J. A. Jonas, A. Jost, Y. Kamae, G. Lohmann, D. J. Lunt, K. H. Nisancioglu, A. Abe-Ouchi, G. Ramstein, C. R. Riesselman, M. M. Robinson, N. A. Rosenbloom, U. Salzmann, C. Stepanek, S. L. Strother, H. Ueda, Q. Yan, and Z.-S. Zhang, Sea Surface Temperature of the mid-Piacenzian Ocean: A Data-Model Comparison, *Sci. Rep.*, vol. 3, 2013; doi:10.1038/srep02013.
- [6] Z.-S. Zhang, K. H. Nisancioglu, M. A. Chandler, A. M. Haywood, B. L. Otto-Bliesner, G. Ramstein, C. Stepanek, A. Abe-Ouchi, W.-L. Chan, F. J. Bragg, C. Contoux, A. M. Dolan, D. J. Hill, A. Jost, Y. Kamae, G. Lohmann, D. J. Lunt, N. A. Rosenbloom, L. E. Sohl, and H. Ueda, Mid-pliocene Atlantic Meridional Overturning Circulation not unlike modern, *Clim. Past*, vol. 9, 1495-1504, 2013b; doi:10.5194/cp-9-1495-2013.
- [7] D. J. Hill, A. M. Haywood, D. J. Lunt, S. J. Hunter, F. J. Bragg, C. Contoux, C. Stepanek, L. Sohl, N. A. Rosenbloom, W.-L. Chan, Y. Kamae, Z.-S. Zhang, A. Abe-Ouchi, M. A. Chandler, A. Jost, G. Lohmann, B. L. Otto-Bliesner, G. Ramstein, and H. Ueda, Evaluating the dominant components of warming in Pliocene climate simulations, *Clim. Past*, vol. 10, 79-90, 2014; doi:10.5194/cp-10-79-2014.
- [8] U. Salzmann, A. M. Dolan, A. M. Haywood, W.-L. Chan, J. Voss, D. J. Hill, A. Abe-Ouchi, B. Otto-Bliesner, F. J. Bragg, M. A. Chandler, C. Contoux, H. J. Dowsett, A. Jost, Y. Kamae, G. Lohmann, D. J. Lunt, S. J. Pickering, M. J. Pound, G. Ramstein, N. A. Rosenbloom, L. Sohl, C. Stepanek, H. Ueda, and Z.-S. Zhang, *Nature Clim. Change*, vol. 3, 969-974, 2013; doi:10.1038/nclimate2008.
- [9] J. R. Stewart, The ecology and adaptation of Neanderthals during the non-analogue environment of Oxygen Isotope Stage 3, *Quat. Int.*, vol. 137, pp. 35-46, 2005; doi:10.1016/j.quatint.2004.11.018.
- [10] S. Manabe and R. J. Stouffer, Coupled ocean-atmosphere model response to freshwater input: Comparison to Younger Dryas event, *Paleoceanography*, vol. 12, pp. 321-336, 1997; doi: 10.1029/96pa03932.
- [11] M. Kageyama, U. Merkel, B. Otto-Bliesner, M. Prange, A. Abe-Ouchi, G. Lohmann, R. Ohgaito, D. M. Roche, J. Singarayer, D. Swingedouw, and X. Zhang, Climatic impacts of fresh water hosing under Last Glacial Maximum conditions: a multi-model study, *Clim. Past*, vol. 9, pp. 935-953, 2013; doi:10.5194/cp-9-935-2013.
- [12] S. Sitch, B. Smith, I. C. Prentice, A. Arneth, A. Bondeau, W. Cramer, J. O. Kaplan, S. Levis, W. Lucht, M. T. Sykes, K. Thonicke, and S. Venevsky, Evaluation of ecosystem dynamics, plant geography and terrestrial carbon cycling in the LPJ dynamic global vegetation model, *Global Change Biol.*, vol. 9, pp. 161-185, 2003; doi:10.1046/j.1365-2486.2003.00569.x.
- [13] S. P. Harrison and M. F. Sanchez Goñi, Global patterns of vegetation response to millennial-scale variability and rapid climate change during the last glacial period, *Quat. Sci. Rev.*, vol. 29, 2957-2980, 2010; doi:10.1016/j.quascirev.2010.07.016.
- [14] G. R. Dickens, J. R. O'Neil, D. K. Rea, and R. M. Owen, Dissociation of oceanic methane hydrate as a cause of the carbon isotope excursion at the end of the Paleocene, *Paleoceanography*, vol. 10, pp. 965-971, 1995.
- [15] S. P. Hesselbo and G. Pienkowski, Stepwise atmospheric carbon-isotope excursion during the Toarcian Oceanic Anoxic Event (Early Jurassic, Polish Basin), *Earth Plan. Res. Lett.*, vol. 301, p.365-372, 2011.
- [16] K-1 model developers: K-1 coupled model (mirc) description. Tech. rep., Center for Climate System Research, The University of Tokyo, 2004.
- [17] E. Piñero, M. Marquardt, C. Hensen, M. Haeckel, K. Wallmann, et al., Estimation of the global inventory of methane hydrates in marine sediments using transfer functions, *Biogeosciences*, vol. 10, pp. 959-975, 2013; doi:10.5194/bg-10-959-2013.
- [18] P. Yiou, J. Servonnat, M. Yoshimori, D. Swingedouw, M. Khodri, A. Abe-Ouchi, Stability of weather regimes during the last millennium from climate simulations. *Geophys. Res. Lett.*, vol. 39, L08703, 2012; doi:10.1029/2012GL051310.
- [19] C. Gao, A. Robock, and C. Ammann, Volcanic forcing of climate over the past 1500 years: An improved ice core-based index for climate models, *J. Geophys. Res.-Atmos.*, vol. 113, p. D23111, 2008.

古環境研究のための多階層数値実験

課題責任者

阿部 彩子 東京大学 大気海洋研究所

著者

阿部 彩子^{*1}, 吉森 正和^{*1}, Wing-Le Chan^{*1}, 山本 彬友^{*1}, 尾崎 和海^{*1}, 大石 龍太^{*2},
市野 美夏^{*2}, 小澤 祐介^{*1}, 小長谷貴志^{*1}, シェリフ多田野サム^{*1}, 新田 友子^{*1}, Alexandre Laine^{*2}

*1 東京大学 大気海洋研究所

*2 情報・システム研究機構 国立極地研究所

大気海洋結合モデル MIROC4m を用いて、温暖な約 3.0 ~ 3.3 百万年前の鮮新世中期 (mPWP)、氷期における千年スケールの寒冷期 (亜氷期)、過去千年 (西暦 850 ~ 2000 年) などの古気候シミュレーションを行った。MIROC4m mPWP シミュレーションでは、低緯度の温暖化には温室効果気体が、高緯度では反射率の低下が重要であることが示された。

また、亜氷期の急激な気候変動と、植生分布への影響を調べるために、淡水流入実験によって得られた境界条件のもとで、大気 GCM と全球動的植生モデルを走らせた。その結果、代替指標によって示される夏の乾燥化をよく再現した。一方で、亜氷期における植生への影響は森林の減少パターンの大局的な変化は再現したが、定量的には過小評価している。

温暖化時におけるメタンハイドレート分解が気候に与える影響を見積もるため、MIROC3.2 を用いて行われた大気二酸化炭素 4 倍増実験結果を用いた初期的な推定を行った。その結果、数千年スケールの時間をかけて多量のメタンハイドレートが分解することが示され、これにより海中の酸素を多量に消費する可能性があることが分かった。

さらに、時間変化する境界条件のもとで、過去千年の気候再現・感度実験も行われた。その結果、極端に大きな火山噴火イベントに対しては太平洋十年規模変動の位相が固定されることが示唆された。この結果は異なる初期値から積分した別のアンサンブルメンバーでも共通して見られた。

キーワード: 大気海洋大循環モデル MIROC, 古気候モデリング, 鮮新世中期, 更新世後期, メタンハイドレート, 過去千年